Journal of *Marine Science and Engineering*

MDPI

Article

Effects of UVR on Photosynthesis in *Sargassum horneri* (Turner) C. Agardh Adapted to Different Nitrogen Levels

Zhiguang Xu [1,2,†], Xiaotong Jiang [1,†], Baoqi Li [1], Zhengzheng Lv [1], Hongyan Wu [1,2], Shasha Zang [1,2], Fang Yan [1,2,*] and Menglin Bao [1,2,*]

[1] School of Life Sciences, Ludong University, Yantai 264025, China
[2] Key Laboratory of Marine Biotechnology in Universities of Shandong, Ludong University, Yantai 264025, China
* Correspondence: yf_dolphin@163.com (F.Y.); mlin0527@163.com (M.B.)
† These authors contributed equally to this work.

Abstract: In recent years, golden tides caused by drifting *Sargassum horneri* (Turner) C. Agardh have caused serious ecological disasters in coastal areas of China. Eutrophication is an important cause of the formation of the golden tide. Additionally, the drifting population on the surface of the ocean is exposed to more ultraviolet radiation (UVR) than the attached population on the sea floor. In this study, the thalli of *S. horneri* were cultivated under two levels of nitrogen (LN: natural seawater, in which the concentration of NO_3^--N was 1 μmol L^{-1}; HN: NO_3^--enriched seawater, in which the concentration of NO_3^--N was 200 μmol L^{-1}) for 6 days with low photosynthetically active radiation (PAR), and then exposed to three levels of radiation (P: photosynthetically active radiation (PAR), 400–700 nm; PA: PAR + UVA, 320–700 nm; PAB: PAR + UVA + UVB, 280–700 nm) under each level of nitrogen for 2 h to investigate the effects of high UVR and nitrogen on photosynthesis. The results showed that the high level of N (HN) only enhanced the synthesis of pigments after 6 days of pre-cultivation under low PAR. After 2 h of high UVR exposure, high P, PA, and PB decreased the maximum photochemical quantum yield (F_v/F_m) and increased non-photochemical quenching (NPQ) in *S. horneri* regardless of the N level, and PAB significantly decreased F_v/F_m compared to PA under the LN condition alone. Under the LN condition, compared to the P group, PA and PAB significantly promoted the synthesis of carotenoids. Under the HN condition, compared to the P group, PAB increased the absorbed flux by active RCs (ABS/RC) and dissipated the energy flux by active RCs (DI_0/RC) in *S. horneri* alone. Furthermore, HN increased F_v/F_m, ABS/RC, and DI_0/RC more in *S. horneri* with PAB in comparison to those in the LN and PAB group. However, no significant differences in these parameters were observed between the LN and HN conditions under the same UVR treatments. These results demonstrate that drifting *S. horneri* on the surface of seawater could be inhibited by the high P; however, *S. horneri* living in eutrophic high-nitrogen seawater may have a stronger ability to resist high UVR damage, especially with regard to PAB radiation, which may be one of the reasons for the formation of golden tides in coastal seawater.

Keywords: *Sargassum horneri*; golden tide; nitrogen; ultraviolet radiation; photosynthesis

Citation: Xu, Z.; Jiang, X.; Li, B.; Lv, Z.; Wu, H.; Zang, S.; Yan, F.; Bao, M. Effects of UVR on Photosynthesis in *Sargassum horneri* (Turner) C. Agardh Adapted to Different Nitrogen Levels. *J. Mar. Sci. Eng.* **2023**, *11*, 498. https://doi.org/10.3390/jmse11030498

Academic Editors: Sang Heon Lee and Azizur Rahman

Received: 15 December 2022
Revised: 17 February 2023
Accepted: 23 February 2023
Published: 25 February 2023

1. Introduction

Golden tides, which are an ecological issue, are caused by the accumulation of large-scale drifting *Sargassum* on the surface of seawater [1]. Recently, golden tides have occurred more frequently, especially in the Mid-Atlantic, Gulf of Mexico, and Caribbean regions [2]. Since 2000, drifting *S. horneri* rafts have also been reported in the East China Sea and the Yellow Sea [3,4]. The outbreak of golden tides has negative ecological and economic impacts on marine life and the activities of human beings [5]. For example, the accumulation of drifting *S. horneri* on the surface of seawater hinders the light and oxygen availability for marine life [6]. In 2016, a golden tide bloomed and moved offshore of Jiangsu Province,

China, which caused serious economic losses due to the reduction in *Neopyropia yezoensis* production, and the economic losses in the seaweed farming industry reached CNY 500 million [7]. The algae that decomposed there was concomitant to the increase in toxic and harmful substances in the seawater, which poses growing effects on coastal ecosystems, such as alterations to seagrasses and benthic fauna on the seafloor, threatening the stability of local ecosystems and affecting the geochemical cycle [8]. Therefore, golden tides have become another major environmental issue after green tides.

Sargassum horneri is the causative species of golden tides in China; it is widely distributed from the Liaodong Peninsula to Guangdong Province and can be observed in eastern and southeastern China [9]. *S. horneri* usually grows abundantly on benthic habitats and is attached to the seafloor through a retainer. the formation of spherical gas-filled bladders in matured *S. horneri* allows the thalli to grow upright from the bottom to the surface of the seawater. When the retainer detaches from the attached matrix, the gas-filled bladders allow the thalli to drift to the surface of the seawater, forming a drifting population [10]. Widespread drifting *S. horneri* invaded the southwest of the Yellow Sea, causing the large-scale golden tides in China. Golden tides even simultaneously occur with a green tide, forming a phenomenon of bimacroalgal tides [11,12].

In recent years, most studies conducted have explored the physiological, ecological, and environmental impacts on *S. horneri*. Bao et al. reported that nutrient limitation and high photosynthetically active radiation (PAR) may accelerate the senescence of *S. horneri* [13]. Some researchers also demonstrated that light is an important factor which affects the outbreak of golden tides, and its influence is more obvious in the drifting process [14]. In addition, it has been reported that UVR has great influences on the growth and physiological and biochemical composition of macroalgae, e.g., it inhibits photosynthesis, damages the synthesis of proteins and photosynthetic pigments, and affects the formation of oxygen radicals [15,16]. Eutrophication in inshore seawater has been regarded as one major cause of algal blooms [1]. Nitrogen (N) is an essential nutrient and a key restrictive nutrient for the growth and development of algae [17]. Most studies have shown that eutrophic high-N seawater could promote the growth rate and photosynthesis of macroalgae by increasing the content of photosynthetic pigments and promoting the activity of the PSII photoreaction system [17]. However, few studies have shown that the growth rate of macroalgae may not be further promoted when the concentration of N in the seawater exceeds the critical level, such as for *Gracilaria lemaneiformis*, but more N would be stored in the algae [18].

To date, we are not aware of any study that has focused on the high P, and coupling effects of high UVR and nitrogen content on the drifting population of *S. horneri*. Thus, in the present study, the thalli of a drifting population of *S. horneri* were exposed to three levels of high radiation and two levels of nitrogen content to explore the photosynthetic response of *S. horneri*, which will provide an important new perspective for the study of the mechanisms of its explosive growth.

2. Materials and Methods

2.1. Materials

Drifting *Sargassum horneri* samples were collected from the coastal water of Rongcheng, Shandong Province, China (37°15′ N, 122°35′ E), and transported to the laboratory in a cooler (4 °C) in 2 h. The dirt and miscellaneous algae on the surface of algal thalli were washed with sterilized natural seawater, and then, healthy and homogeneous branches were selected and cultured with sterilized natural seawater in growth chambers (MGC-250P, Yiheng Technical Co., Ltd., Shanghai, China) for 24 h. The temporary culture conditions were as follows: temperature of 18 °C, 80 μmol photons m^{-2} s^{-1} of photosynthetic active radiation (PAR), and a light and dark period of 12 h:12 h. The stocking density was about 2 g L^{-1}, and the media were continuously aerated at a rate of 2 L min^{-1}.

2.2. Experimental Design

After temporary culture, the thalli were adapted to two different N levels for 6 days. Two N concentrations were set: the low N condition (LN, natural seawater; the concentration of NO_3-N was 1 μmol L^{-1}) and the high N condition (HN, with the addition of 200 μmol L^{-1} of $NaNO_3$ to natural seawater). The nitrogen content of 50 μmol L^{-1} in natural seawater was observed in the sampling sites, and in previous research, it was reported that the inorganic nitrogen content in golden tide bloom area increased by 3–4 times [19]. In all the treatments, the concentration of inorganic phosphorus (P) was set to 10 μmol L^{-1} through the addition of KH_2PO_4 to avoid P limitation [20,21]. Other conditions were the same as the temporary culture, and the seawater medium was renewed every two days.

The maximum photochemical quantum yield (F_v/F_m) of the algae was measured every day to ensure that the algae were in a healthy state. The F_v/F_m of the algae was in a relatively stable state after continuous culture for 6 days, and then, thalli adapted to low and high N levels were randomly selected and exposed to three radiation conditions: P (PAR, 400–700 nm, 700 μmol photons m^{-2} s^{-1}), PA (PAR + UVA, 320–700 nm, PAR: 700 μmol photons m^{-2} s^{-1}; UVA: 36.2 W m^{-2}), or PAB (PAR + UVA + UVB, 280–700 nm, PAR: 700 μmol photons m^{-2} s^{-1}; UVA: 36.2 W m^{-2}; UVB: 1.2 W m^{-2}) [22] for 2 h. Algal samples from each nitrogen condition without radiation treatment were used as a control group. In this study, three replications of each treatment were performed. Light was provided by a solar simulator (Sol 1200, Hönle GmbH, Martinsried, Germany; the emission spectrum is shown in Figure 1), and different radiations were obtained by covering quartz tubes with different types (ZJB-400, ZJB-320, and ZJB-280) of optical filters (Nantong Yinxing Optical Co., Ltd., Nantong, China). During culture, the quartz tubes with thalli were placed in a water bath, and the temperature was controlled at 18 °C by a low-temperature thermostatic bath (YRDC-0506, Shanghai Yarong Biochemical Instrument Co., Ltd, Shanghai, China). Photosynthetic physiological characteristics of the algae, such as F_v/F_m, rapid light curve, non-photochemical quenching (NPQ), OJIP polyphasic chlorophyll *a* fluorescence rise kinetics, contents of photosynthetic pigments, and the nitrate reductase activity (NRA), were measured before and after the different radiation treatments.

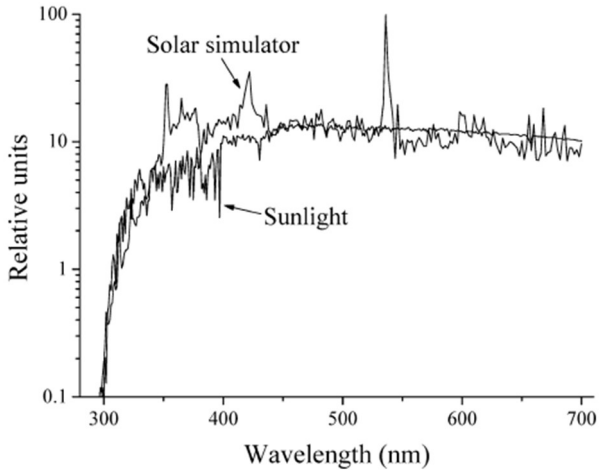

Figure 1. The emission spectrum of the solar simulator which provides culture light.

2.3. Determination of F_v/F_m and NPQ

Algal thalli in good condition were sampled and adapted to dark conditions for 5 min, and the chlorophyll fluorescence parameters were measured using a handheld chlorophyll fluorescence meter (AP-C100, Photon Systems Instruments, Brno, Czech Republic). The algae were first irradiated with a light source of low irradiance (approximately 0.15 μmol photons m^{-2} s^{-1}) to obtain the minimum fluorescence (F_0) in dark adaptation, and then, saturated light (4000 μmol photons m^{-2} s^{-1}) was used to obtain the maximum

fluorescence (F_m) in the dark-adapted state. Finally, the maximum fluorescence (F_m') of the algae in the light-adapted state was measured using saturated light.

$$\text{The maximum photochemical quantum yield of PSII: } F_v/F_m = (F_m - F_0)/F_m$$

$$\text{Non-photochemical quenching: NPQ} = (F_m - F_m')/F_m$$

2.4. Acquisition of Rapid Light Response Curves

After 5 min of dark adaptation, the rapid light curves (RLCs) of the algal samples were measured using a modulated chlorophyll fluorescence instrument (FL6000, Photon Systems Instruments, Brno, Czech Republic). The selected LC3 program contains 7 gradients of photochemical light: 10, 20, 50, 100, 300, 500, and 1000 µmol photons m^{-2} s^{-1}. Each gradient lasted 1 min. The quantum yield was measured, and the relative electron transport rate (rETR) was calculated as follows [23]:

$$\text{Relative electron transport rate rETR (II)} = \Phi\text{PSII} \times \text{PFD} \times 0.5,$$

where PSII is the actual light quantum yield of PSII, PFD is the actinic light intensity, and 0.5 is the ratio of absorbed light via PSII to the total incident light.

The maximum relative electron transport rate ($rETR_{max}$) and the initial slope (α) were obtained by fitting the data to a non-linear function as shown in the following formula [24,25]:

$$\text{rETR} = \text{rETR}_{max} \times \tanh(\alpha \times \text{PAR}/\text{rETR}_{max})$$

$$\text{Minimum saturation irradiance } E_k = \text{rETR}_{max}/\alpha$$

2.5. Determination of Rapid Chlorophyll Fluorescence Induction and JIP Test

Sargassum horneri samples were adapted to dark conditions for 5 min, and the rapid chlorophyll fluorescence induction and JIP test was carried out using a double-modulated chlorophyll fluorescence instrument (FL6000, Photon Systems Instruments, Brno, Czech Republic). The fluorescence signals were recorded with a scanning time that ranged from 10 µs to 2 s and were labeled as O, J (at about 2 ms), I (at about 30 ms), and P. In order to show the obvious OJIP phase, the horizontal coordinate time was changed to a logarithmic form to directly observe the J and I points and infer the state of the PSII reaction center. In the rapid chlorophyll fluorescence induction kinetic curve (OJIP curve), light energy was absorbed by the excited antenna pigment (ABS, absorbed light energy). The excited energy was captured (TR) and transferred to the reaction center (RC), and the rest was dissipated in the form of heat or fluorescence. V_J reflects the degree of closure of the reaction center at 2 ms, and M_0 reflects the maximum rate at which QA was restored. Ψ_0 reflects the possibility of electron transport beyond Q_A.

The relevant parameters were calculated as follows [26]:

$$V_J = (F_{2ms} - F_0)/(F_m - F_0)$$

$$M_0 = 4 \times (F_{300\mu s} - F_0)/(F_m - F_0)$$

$$\Psi_0 = 1 - V_J$$

$$\text{ABS/RC} = M_0 \times (1/V_J) \times [F_m/(F_m - F_0)]$$

$$\text{TR}_0/\text{RC} = M_0 \times (1/V_J)$$

$$\text{ET}_0/\text{RC} = M_0 \times (1/V_J) \times \Psi_0$$

$$\text{DI}_0/\text{RC} = (\text{ABS/RC}) - (\text{TR}_0/\text{RC})$$

2.6. Determination of Photosynthetic Pigments

The determination of pigments was carried out by referring to the method reported by Wellburn [27]. About 0.2 g of fresh-weight (FW) thalli was placed in a mortar with 10 mL of methanol solution, and then, it was ground into a homogeneous slurry. After 24 h of dark extraction in a 4 °C refrigerator, the extract solution was centrifuged for 10 min at 4 °C and 5000 r min^{-1} using a high-speed refrigerated centrifuge. The absorbance values of the supernatant were scanned by using a UV spectrophotometer at a wavelength of 280~750 nm. The contents of photosynthetic pigments were calculated using the following formula:

$$\text{Chlorophyll } a \text{ (mg g}^{-1}) = [16.29 \times (A_{665} - A_{750}) - 8.54 \times (A_{652} - A_{750})] \times V/(FW \times 1000)$$

$$\text{Carotenoid (mg g}^{-1}) = 7.6 \times [(A_{480} - A_{750}) - 1.49 \times (A_{510} - A_{750})] \times V/(FW \times 1000)$$

where A_{470}, A_{653}, A_{666}, and A_{750} is the absorbance at 470 nm, 653 nm, 666 nm, and 750 nm, respectively.

2.7. Determination of Nitrate Reductase Activity (NRA)

Referring to the method reported by Corzo and Niell [28], approximately 0.1 g of FW thalli were incubated in the reaction solution (10 mL) for 1 h at 30 °C in the dark. The reaction solution was prepared as follows: 0.1 mol L^{-1} phosphate buffer, pH 7.5; 1 mmol L^{-1} EDTA; 0.1% propanol; 0.2 mol L^{-1} $NaNO_3$; 10 µmol L^{-1} glucose. The O_2 in the solution was removed by filling N_2 for 2 min to prevent the generated NO_2^- from being oxidized to NO_3^- before the incubation. The reaction was terminated by removing the algae from the solution, and the concentration of NO_2^- produced in the solution was determined. The concentration of NO_2^- produced was determined colorimetrically at 540 nm [29]. The activity of nitrate reductase was expressed as µmol NO_2^- g^{-1} FW h^{-1}.

2.8. Statistical Analysis of Data

All the measurement results were expressed as mean ± standard deviation ($n \geq 3$). The data were analyzed using the Prism 7.0 and SPSS v.20 software. A two-way ANOVA (Duncan) was conducted to analyze the interactive effects of UVR and N levels on F_v/F_m, $rETR_{max}$, α, E_k, NPQ, OJIP curve, photosynthetic pigments, and nitrate reductase activity (NRA). The significance level was set as $p < 0.05$, and different lowercase letters represent significant differences among the different treatments.

3. Results

3.1. Maximum Photochemical Quantum Yield (F_v/F_m)

In the process of pre-cultivation, under the HN condition, the F_v/F_m of *Sargassum horneri* significantly decreased on day 2, rebounded on day 3, and then remained stable (around 0.6) during the subsequent culture process from day 3 to day 6. Under the LN condition, the F_v/F_m of *S. horneri* remained stable during the 6-day cultivation period, which was about 0.6 (Figure 2A).

UVR had an independent effect on the F_v/F_m of *S. horneri* ($p < 0.05$), the N concentration had no effect on F_v/F_m ($p > 0.05$), and there was no interactive effect between UVR and N levels on F_v/F_m ($p > 0.05$) (Figure 2B). The F_v/F_m of *S. horneri* was not affected by HN after 6 days of pre-cultivation ($p > 0.05$) (Figure 2B). After 2 h of UVR exposure, under the LN condition, the F_v/F_m of *S. horneri* was the lowest during the PAB treatment with 0.36 and highest during the PA treatment with 0.54 ($p < 0.05$) (Figure 2B). Compared to the P group, the F_v/F_m of *S. horneri* under the PA and PAB conditions were not significantly different ($p > 0.05$) (Figure 2B). There was no significant difference among different UVR treatments under the HN condition ($p > 0.05$). The F_v/F_m of *S. horneri* increased by 3% and 32% when treated with PA and PAB under HN compared to those treated with the same UVR under the LN condition, respectively ($p > 0.05$) (Figure 2B).

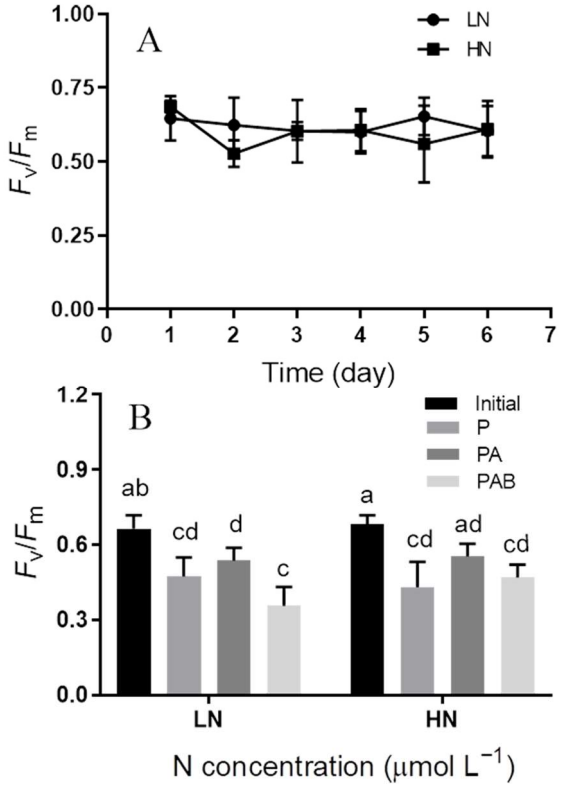

Figure 2. F_v/F_m of *Sargassum horneri* in the 6-day pre-cultivation period (**A**) and after 2 h of exposure to P, PA, and PAB (**B**). Significant differences among all treatments are indicated by different lowercase letters ($p < 0.05$).

3.2. Rapid Light Curve and Non-Photochemical Quenching

Both the UVR and N levels were found to have no significant effects on the α, $rETR_{max}$, and E_k of *S. horneri* ($p > 0.05$), and there was no interaction effect between the UVR and N concentration on them ($p > 0.05$) (Table 1). After 6 days of pre-cultivation, the α and $rETR_{max}$ of *S. horneri* were not affected by HN ($p > 0.05$), but HN decreased the E_k of *S. horneri* more than LN did ($p < 0.05$) (Table 1). After 2 h of UVR exposure, a significant difference was only found in the $rETR_{max}$ between the HN and P group (85.41 ± 25.07) and the LN and P group (52.89 ± 18.59) ($p < 0.05$), and the $rETR_{max}$ of *S. horneri* was highest in the P and HN group among all treatments (Table 1 and Figure 3).

Table 1. Photosynthetic parameters of rapid light curve for *Sargassum horneri* cultured under different treatments. α is the electron transport efficiency, $rETR_{max}$ is the maximum relative electron transport rate, and E_k is the minimum saturated irradiance. Different superscript letters indicate significant differences among different treatments ($p < 0.05$).

		α	**$rETR_{max}$** **μmol e^- m^{-2} s^{-1}**	**E_k**
Initial	LN	0.24 ± 0.05 ^{a}	57.11 ± 18.36 ^{ab}	232.15 ± 42.65 ^{ab}
	HN	0.24 ± 0.06 ^{a}	45.41 ± 13.67 ^{a}	188.88 ± 36.07 ^{a}
P	LN	0.21 ± 0.05 ^{a}	52.89 ± 18.59 ^{a}	248.03 ± 49.10 ^{ab}
	HN	0.30 ± 0.06 ^{a}	85.41 ± 25.07 ^{b}	277.58 ± 33.44 ^{ab}
PA	LN	0.25 ± 0.09 ^{a}	55.24 ± 8.75 ^{ab}	232.52 ± 59.54 ^{ab}
	HN	0.21 ± 0.07 ^{a}	67.46 ± 4.94 ^{ab}	344.44 ± 99.36 ^{b}
PAB	LN	0.24 ± 0.06 ^{a}	63.55 ± 20.15 ^{ab}	277.77 ± 105.03 ^{ab}
	HN	0.26 ± 0.05 ^{a}	57.98 ± 13.60 ^{ab}	227.24 ± 62.02 ^{ab}

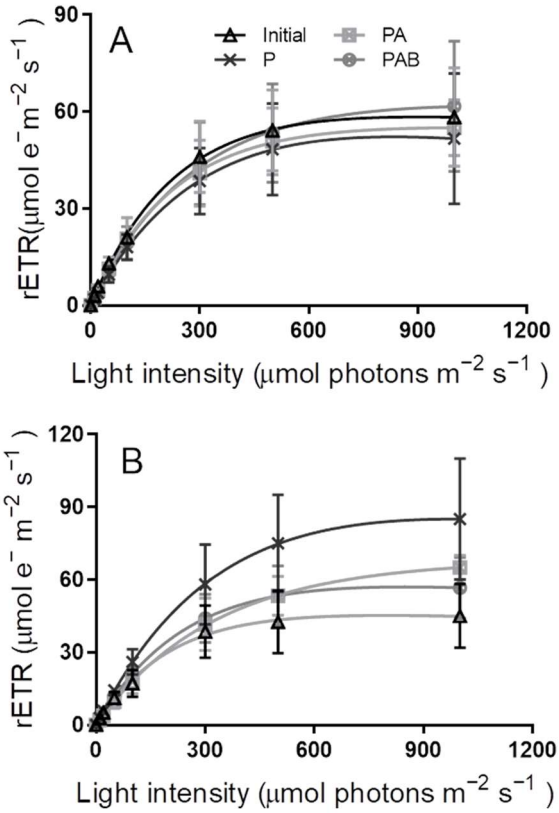

Figure 3. The electron transport rates of *Sargassum horneri* with LN (**A**) and HN (**B**) under P, PA, and PAB treatments.

UVR only had a main effect on the NPQ of *S. horneri* ($p < 0.05$) (Figure 4), N levels had no main effect on the NPQ of *S. horneri* ($p > 0.05$) (Figure 4), and there was no interaction effect between these two factors ($p > 0.05$) (Figure 4). After 6 days of pre-cultivation, HN did not enhance the NPQ of *S. horneri* ($p > 0.05$) (Figure 4). The NPQ of *S. horneri* treated using UVR was significantly higher than the initial values of NPQ regardless of N levels ($p < 0.05$), and a significant difference did not occur among different UVR and N treatments after 2 h of UVR exposure ($p > 0.05$) (Figure 4).

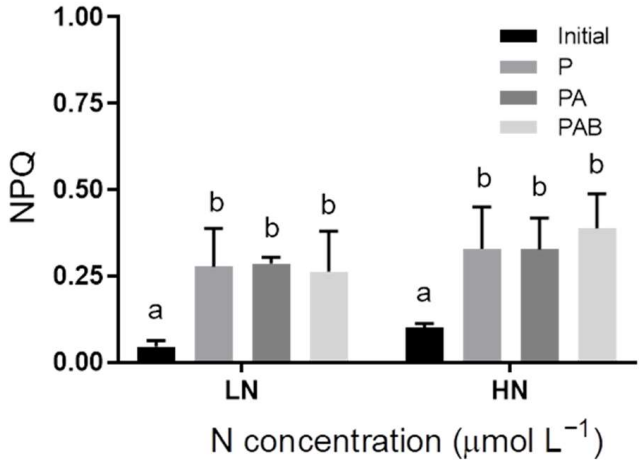

Figure 4. Non-photochemical quenching (NPQ) of *Sargassum horneri* under P, PA, and PAB treatments. Significant differences among all treatments are indicated by different lowercase letters ($p < 0.05$).

3.3. OJIP Curve

Typical OJIP curves with different treatments are shown in Figure 5. UVR was found to have significant effects on the V_J, M_0, Ψ_0, ABS/RC, DI_0/RC, ET_0/RC, and TR_0/RC of *S. horneri* ($p < 0.05$) (Figures 6 and 7), while N levels had no significant effect on these parameters, as described above ($p > 0.05$) (Figures 6 and 7). There were no interaction effects between the UVR and N levels on these parameters ($p > 0.05$) (Figures 6 and 7). The V_J, M_0, and Ψ_0 of *S. horneri* were not significantly enhanced under HN after 6 days of pre-cultivation ($p > 0.05$) (Figure 6). The V_J and M_0 of *S. horneri* increased after 2 h of UVR exposure in comparison to the initial group, especially in the HN condition ($p < 0.05$) (Figure 6A,B). There was no significant difference in V_J among all the UVR and N treatments, but the values of V_J in samples treated using PAB reached a maximum of 0.79 under LN and a maximum of 0.78 under HN (Figure 6A). Like V_J, the M_0 of *S. horneri* treated using PAB reached a maximum of 1.28 under LN and 1.16 under HN (Figure 6B). The change in Ψ_0 was opposite to that of V_J and M_0 under the same conditions, and its lowest value was 0.21 under LN and 0.22 under HN after PAB treatment ($p < 0.05$) (Figure 6C).

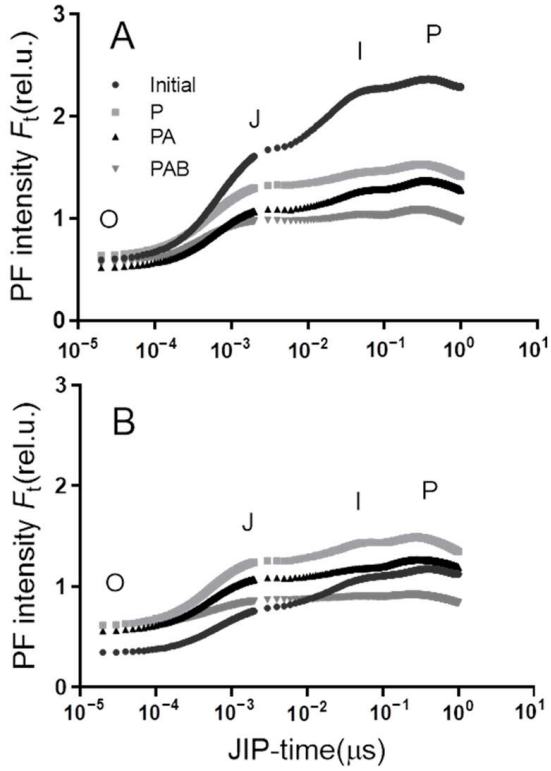

Figure 5. Chlorophyll *a* fluorescence transients (OJIP) of *Sargassum horneri* under LN (**A**) and HN (**B**) under P, PA, and PAB treatments.

The changes in the ABS/RC and DI_0/RC of *S. horneri* showed the same trends (Figure 7B,C). Under LN, no significant difference was found regarding the ABS/RC and DI_0/RC of *S. horneri* among all the treatments, including the initial group. However, under the HN condition, the ABS/RC and DI_0/RC of *S. horneri* were significantly higher under the PAB condition than in both the P and PA groups ($p < 0.05$) (Figure 7B,C). HN did not affect ABS/RC and DI_0/RC under the same UVR conditions ($p > 0.05$) (Figure 7B,C). In terms of ET_0/RC, under the LN condition, it was only significantly lower under the PAB condition and not under the initial condition ($p < 0.05$). However, under HN, the ET_0/RC of *S. horneri* was significantly lower during all three different UVR treatments than that during the initial condition ($p < 0.05$). After 2 h of UVR exposure, there was no significant difference regarding ET_0/RC among the different UVR treatments at the same N concentration ($p > 0.05$) (Figure 7C).

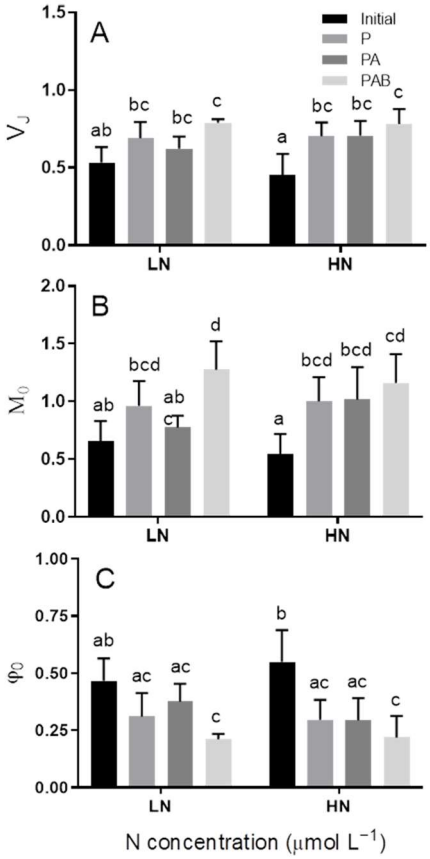

Figure 6. V_J (**A**), M_0 (**B**), and Ψ_0 (**C**) of *Sargassum horneri* under P, PA, and PAB treatments. Significant differences among all treatments are indicated by different lowercase letters ($p < 0.05$).

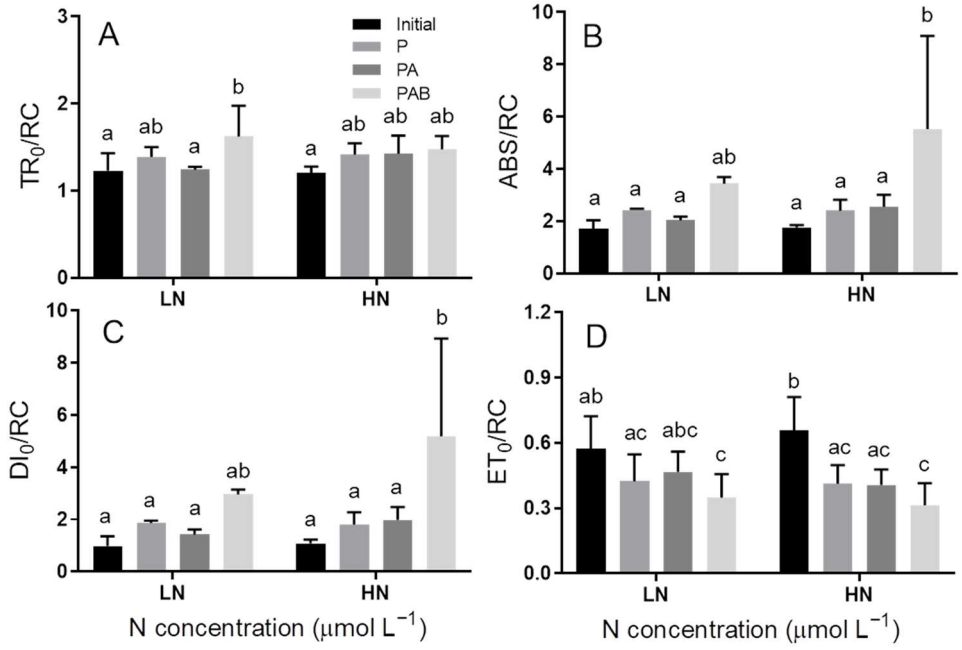

Figure 7. TR_0/RC (**A**), ABS/RC (**B**), DI_0/RC (**C**), and ET_0/RC (**D**) of *Sargassum horneri* under P, PA, and PAB treatments. Significant differences among all treatments are indicated by different lowercase letters ($p < 0.05$).

3.4. Pigment Contents

Both the UVR and N levels had main effects on chlorophyll *a* and carotenoids in *S. horneri* ($p < 0.05$), but there was no interaction effect between the UVR and N levels on chlorophyll *a* and carotenoids in *S. horneri* ($p > 0.05$) (Figure 8A,B). After 6 days of pre-cultivation, an enhancement of chlorophyll *a* and carotenoid contents in *S. horneri* was observed in the HN condition. After 2 h of UVR exposure, under LN, significant increases in the contents of chlorophyll *a* and carotenoids were observed in the PA and PAB treatments in comparison to the initial group ($p < 0.05$) (Figure 8A,B). However, under HN, no significant differences in the contents of chlorophyll *a* and carotenoids were found among all the groups, including the initial group ($p > 0.05$) (Figure 8A,B).

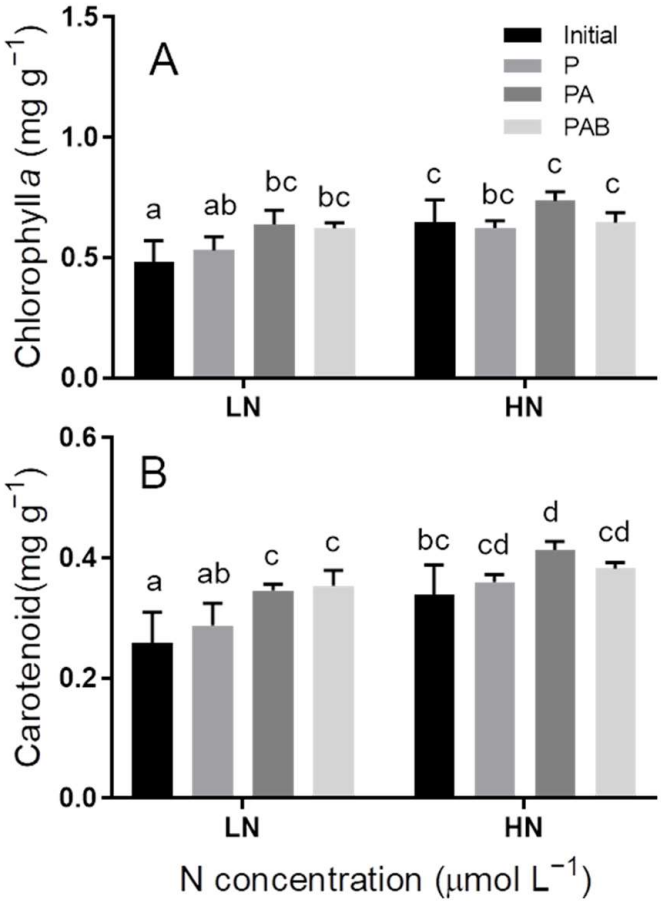

Figure 8. Chlorophyll *a* (**A**) and carotenoids (**B**) of *Sargassum horneri* under P, PA, and PAB treatments. Significant differences among all treatments are indicated by different lowercase letters ($p < 0.05$).

3.5. The Nitrate Reductase Activity (NRA)

The UVR and N levels had an interactive effect on the NRA of *S. horneri* ($p < 0.05$), and each factor had main effects on it ($p < 0.05$) (Figure 9). HN had no positive effect on NRA after 6 days of pre-cultivation. After 2 h of UVR exposure, the values of the NRA of *S. horneri* in the LN and P group were significantly higher than the NRA in other groups ($p < 0.05$) (Figure 9), and no significant difference was observed among all groups, except for the LN and P group ($p > 0.05$) (Figure 9).

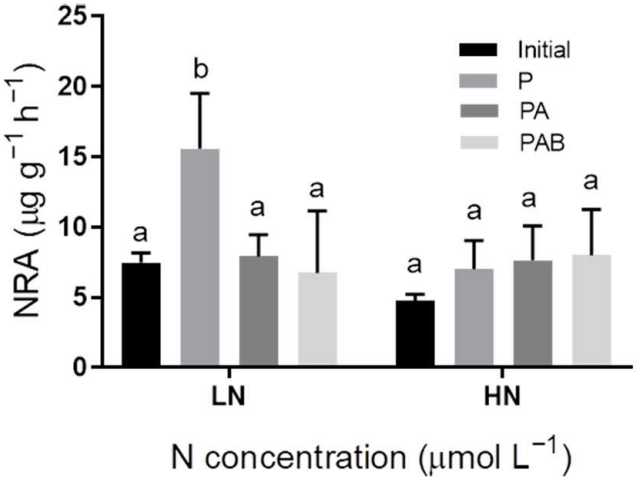

Figure 9. NRA of *Sargassum horneri* under P, PA, and PAB treatments. Significant ($p < 0.05$) differences among the treatments are indicated by different lowercase letters.

4. Discussion

Sargassum horneri drifting on the surface of seawater are easier to expose to high levels of UVR. Decreased F_v/F_m and increased NPQ were observed when algae were exposed to high P level than low P. Our results suggest that *S. horneri* alleviate the inhibitory effects of high P by increasing NPQ. Previous research also demonstrated that drifting *S. horneri* have evolved a range of mechanisms to adapt to high radiation on the surface of seawater, and algae adapts to high radiation stress via physiological regulation, such as the consumption of excess light energy [30,31]. Excess energy dissipates as heat increases to relieve the excitation pressure and keep cells in a normal state [32]. Under the high P condition, the increase in NRA could improve the activity of nitrate utilization to provide a bigger N source; however, limiting N could not significantly increase the synthesis of chlorophyll *a* and carotenoids. Carotenoids play an important role in protecting algae from UVR [33]. When exposed to high PA and PAB, a significant increase in content of carotenoids in *S. horneri* was observed in our study, suggesting that PA and PAB could promote carotenoid synthesis and protect algae from the damage of UVR. Similar results were reported regarding *Chondrus Crispus* [34]. Even though the damage of PAB was considered more severe than that of PA, in this study, the lowest F_v/F_m was found in the PAB condition with low N content.

More studies have mentioned the interactive effects of PA (or PAB) and other environmental factors on macroalgae. When nitrogen was enriched, HN could provide more metabolic expenses for the synthesis of photosynthetic pigments and carotenoids at low P and high P and PA conditions; these results show that HN could improve photosynthetic activity and the ability of photoprotection. The changing contents of chlorophylls and carotenoids are important photoprotection mechanisms in algae [35–37]. When exposed to PAB, compared to the PA condition, PAB decreased F_v/F_m in the same LN condition but did not significantly inhibit F_v/F_m in the same HN condition; these results suggest that HN may increase the tolerance to high PAB in *S. horneri*.

The OJIP curve can reflect the electron transport rate on the donor side and the recipient side of PSII [38] and reflect the initial reaction of photosynthesis. In this study, the Ψ_0 significantly decreased after 2 h of high PAB exposure. This result indicates that high PAB may damage the acceptor region of the PSII protein of *S. horneri*. At the same time, an increase in V_J was also observed after high PAB exposure, suggesting the enhancement of closed PSII reaction center levels. The results in this study show that PAB could rapidly increase the fluorescence value and hinder the electron transfer from Q_A^- to Q_B in algae cells, leading to the accumulation of Q_A^- [26,38–40]. As a result, high P, PA, and PAB levels had inhibitory effects on algae. Furthermore, PAB enhanced the inhibition of the oxidation

of Q_A^-, resulting in the highest V_J in both the LN and HN conditions. PAB also increased the ABS/RC and DI_0/RC levels but still decreased the ET_0/RC levels; these results show that the energy used for electron transfer is reduced and the electron transfer from Q_A^- to Q_B is blocked, which may cause the generation of non-Q_B reduction centers in PSII systems, inhibiting photosynthesis [38,41]. ABS/RC and DI_0/RC were further improved by PAB in the HN condition, but there was no obvious difference regarding TR_0/RC between the LN and HN group with PAB. PAB radiation increases the light energy absorbed by the unit reaction center in the PSII system, but the algae may maintain the normal state of the PSII system by increasing the heat energy dissipation [42], which is more significant in the HN environment. Hence, the algae could more effectively maintain PSII activity against PAB stress in the HN condition.

Here, we found that high PAB obviously reduced the activity of *S. horneri* and inhibited the photosynthesis process of *S. horneri*. In this study, the high N concentration could not completely offset the radiation damage; however, a high N concentration could increase the synthesis of pigments, change the activity of the PSII reaction center, and increase the maximum photosynthetic capacity. Therefore, it is speculated that eutrophic seawater is more prone to the occurrence of golden tides, because nitrogen is the key factor in the growth of algae, and the higher availability of nitrogen sources could improve the protective ability of algae under ultraviolet stress.

Author Contributions: Data curation, X.J.; Formal analysis, B.L. and Z.L.; Funding acquisition, Z.X. and F.Y.; Methodology, H.W.; Software, S.Z.; Validation, F.Y.; Writing—original draft, Z.X.; Writing—review and editing, F.Y. and M.B. All authors have read and agreed to the published version of the manuscript.

Funding: This study was funded by the National Natural Science Foundation of China (Nos. 42276119, 42206106, and 42076206), Shandong Provincial Natural Science Foundation (ZR2020MD092), and Guangdong Basic and Applied Basic Research Foundation (2020A1515011073).

Institutional Review Board Statement: Not applicable.

Informed Consent Statement: Not applicable.

Data Availability Statement: The datasets generated and/or analyzed during the current study are available from the corresponding author on reasonable request.

Conflicts of Interest: The authors declare no conflict of interest.

References

1. Smetacek, V.; Zingone, A. Green and golden seaweed tides on the rise. *Nature* **2013**, *504*, 84–88. [CrossRef]
2. Van Alstyne, K.L.; Nelson, T.; Ridgway, R.L. Environmental Chemistry and Chemical Ecology of "Green Tide" Seaweed Blooms. *Integr. Comp. Biol.* **2015**, *55*, 518–532. [CrossRef] [PubMed]
3. Teichberg, M.; Fox, S.E.; Olsen, Y.S.; Valiela, I.; Martinetto, P.; Iribarne, O.; Muto, E.Y.; Petti, M.A.V.; Corbisier, T.N.; Soto-Jimenez, M.F.; et al. Eutrophication and macroalgal blooms in temperate and tropical coastal waters: Nutrient enrichment experiments with Ulva spp. *Glob. Change Biol.* **2010**, *16*, 2624–2637. [CrossRef]
4. Zhang, J.H.; Shi, J.T.; Gao, S.; Huo, Y.Z.; Cui, J.J.; Shen, H.; Liu, G.Y.; He, P.M. Annual patterns of macroalgal blooms in the Yellow Sea during 2007–2017. *PLoS ONE* **2019**, *14*, e0210460. [CrossRef]
5. Zingone, A.; Enevoldsen, H.O. The diversity of harmful algal blooms: A challenge for science and management. *Ocean Coast. Manag.* **2000**, *43*, 725–748. [CrossRef]
6. Norkko, J.; Bonsdorff, E.; Norkko, A. Drifting algal mats as an alternative habitat for benthic invertebrates: Species specific responses to a transient resource. *J. Exp. Mar. Biol. Ecol.* **2000**, *248*, 79–104. [CrossRef]
7. Xing, Q.G.; Guo, R.H.; Wu, L.L.; An, D.Y.; Cong, M.; Qin, S.; Li, X.R. High-Resolution Satellite Observations of a New Hazard of Golden Tides Caused by Floating Sargassum in Winter in the Yellow Sea. *IEEE Geosci. Remote Sens. Lett.* **2017**, *14*, 1815–1819. [CrossRef]
8. Xiao, J.; Wang, Z.L.; Liu, D.Y.; Fu, M.Z.; Yuan, C.; Yan, T. Harmful macroalgal blooms (HMBs) in China's coastal water: Green and golden tides. *Harmful Algae* **2021**, *107*, 102061. [CrossRef]
9. Wu, H.L.; Feng, J.C.; Li, X.S.; Zhao, C.Y.; Liu, Y.H.; Yu, J.T.; Xu, J.T. Effects of increased CO_2 and temperature on the physiological characteristics of the golden tide blooming macroalgae *Sargassum horneri* in the Yellow Sea, China. *Mar. Pollut. Bull.* **2019**, *146*, 639–644. [CrossRef] [PubMed]
10. Hinojosa, I.; Pizarro, M.; Ramos, M.; Thiel, M. Spatial and temporal distribution of floating kelp in the channels and fjords of southern Chile. *Estuar. Coast. Shelf Sci.* **2010**, *87*, 367–377. [CrossRef]

11. Liu, F.; Liu, X.; Wang, Y.; Jin, Z.; Moejes, F.W.; Sun, S. Insights on the *Sargassum horneri* golden tides in the Yellow Sea inferred from morphological and molecular data. *Limnol. Oceanogr.* **2018**, *63*, 1762–1773. [CrossRef]
12. Xiao, J.; Wang, Z.L.; Song, H.J.; Fan, S.L.; Yuan, C.; Fu, M.Z.; Miao, X.X.; Zhang, X.L.; Su, R.G.; Hu, C.M. An anomalous bi-macroalgal bloom caused by Ulva and Sargassum seaweeds during spring to summer of 2017 in the western Yellow Sea, China. *Harmful Algae* **2020**, *93*, 101760. [CrossRef]
13. Bao, M.; Park, J.-S.; Wu, H.; Lee, H.J.; Park, S.R.; Kim, T.-H.; Son, Y.B.; Lee, T.H.; Yarish, C.; Kim, J.K. A comparison of physiological responses between attached and pelagic populations of *Sargassum horneri* under nutrient and light limitation. *Mar. Environ. Res.* **2022**, *173*, 105544. [CrossRef] [PubMed]
14. Qi, L.; Hu, C.M.; Wang, M.Q.; Shang, S.L.; Wilson, C. Floating Algae Blooms in the East China Sea. *Geophys. Res. Lett.* **2017**, *44*, 11501–11509. [CrossRef]
15. Atienzar, F.A.; Cordi, B.; Donkin, M.E.; Evenden, A.J.; Jha, A.N.; Depledge, M.H. Comparison of ultraviolet-induced genotoxicity detected by random amplified polymorphic DNA with chlorophyll fluorescence and growth in a marine macroalgae, Palmariapalmata. *Aquat. Toxicol.* **2000**, *50*, 1–12. [CrossRef] [PubMed]
16. Hollósy, F. Effects of ultraviolet radiation on plant cells. *Micron* **2001**, *33*, 179–197. [CrossRef]
17. Yu, J.; Li, J.Y.; Wang, Q.H.; Liu, Y.; Gong, Q.L. Growth and Resource Accumulation of Drifting *Sargassum horneri* (Fucales, Phaeophyta) in Response to Temperature and Nitrogen Supply. *J. Ocean Univ. China* **2019**, *18*, 1216–1226. [CrossRef]
18. Yu, J.; Yang, Y.-F. Physiological and biochemical response of seaweed *Gracilaria lemaneiformis* to concentration changes of N and P. *J. Exp. Mar. Biol. Ecol.* **2008**, *367*, 142–148. [CrossRef]
19. Wang, M.; Hu, C.; Barnes, B.B.; Mitchum, G.; Lapointe, B.; Montoya, J.P. The great Atlantic Sargassum belt. *Science* **2019**, *365*, 83–87. [CrossRef] [PubMed]
20. Wu, H.; Li, X.; Liu, Y.; Wang, C.; Ji, C.; Xu, J. Increased Temperature and Nitrogen Enrichment Inhibit the Growth of the Golden Tide Blooming Macroalgae *Sargassum horneri* in the Yellow Sea, China. *J. Mar. Sci. Eng.* **2022**, *10*, 1692. [CrossRef]
21. Ding, G.; Yu, X.Q.; Zhan, D.M.; Zhang, S.C.; Lu, X.; Li, M.Z.; Wu, H.Y. Effects of nitrogen and phosphorus concentrations and ratio on growth in sea weed *Sargassum thunbergii* seedlings. *Fish. Sci.* **2014**, *33*, 219–222. [CrossRef]
22. Rumyantseva, A.S.; Henson, S.A.; Martin, A.P.; Thompson, A.F.; Damerell, G.M.; Kaiser, J.; Heywood, K.J. Phytoplankton spring bloom initiation: The impact of atmospheric forcing and light in the temperate North Atlantic Ocean. *Prog. Oceanogr.* **2019**, *178*, 102202. [CrossRef]
23. Genty, B.; Briantais, J.-M.; Baker, N.R. The relationship between the quantum yield of photosynthetic electron transport and quenching of chlorophyll fluorescence. *Biochim. Biophys. Acta (BBA) Gen. Subj.* **1989**, *990*, 87–92. [CrossRef]
24. Jassby, A.D.; Platt, T. Mathematical formulation of the relationship between photosynthesis and light for phytoplankton. *Limnol. Oceanogr.* **1976**, *21*, 540–547. [CrossRef]
25. Henley, W.J. Measurement and interpretation of photosynthetic light-response curves in algae in the context of photoinhibition and diel changes. *J. Phycol.* **1993**, *29*, 729–739. [CrossRef]
26. Strasser, R.J.; Srivastava, A.; Tsimilli-Michael, M. The fluorescence transient as a tool to characterize and screen photosynthetic samples. In *Probing Photosynthesis: Mechanisms Regulation and Adaptation*; Yunus, M., Pathre, U., Mohanty, E., Eds.; Taylor and Francis: London, UK, 2000; pp. 445–483.
27. Wellburn, A.R. The Spectral Determination of Chlorophylls a and b, as well as Total Carotenoids, Using Various Solvents with Spectrophotometers of Different Resolution. *J. Plant Physiol.* **1994**, *144*, 307–313. [CrossRef]
28. Corzo, A.; Niell, F.X. Determination of nitrate reductase activity in Ulva rigida C. Agardh by the in situ method. *J. Exp. Mar. Biol. Ecol.* **1991**, *146*, 181–191. [CrossRef]
29. Wang, Q.-H.; Yu, L.-J.; Liu, Y.; Lin, L.; Lu, R.-G.; Zhu, J.-P.; He, L.; Lu, Z.-L. Methods for the detection and determination of nitrite and nitrate: A review. *Talanta* **2017**, *165*, 709–720. [CrossRef]
30. Koch, K.; Thiel, M.; Hagen, W.; Graeve, M.; Gómez, I.; Jofre, D.; Hofmann, L.C.; Tala, F.; Bischof, K. Short- and long-term acclimation patterns of the giant kelp *Macrocystis pyrifera* (Laminariales, Phaeophyceae) along a depth gradient. *J. Phycol.* **2016**, *52*, 260–273. [CrossRef]
31. Nan, G.N.; Zhang, Q.S.; Sheng, Z.T.; Zhang, D. Coordination between xanthophyll cycle and antioxidant system in *Sargassum thunbergii* (Sargassaceae, Phaeophyta) in response to high light and dehydration stresses. *J. Appl. Phycol.* **2016**, *28*, 2587–2596. [CrossRef]
32. Gururani, M.A.; Venkatesh, J.; Tran, L.S.P. Regulation of Photosynthesis during Abiotic Stress-Induced Photoinhibition. *Mol. Plant* **2015**, *8*, 1304–1320. [CrossRef]
33. Rao, M.V.; Paliyath, G.; Ormrod, D.P. Differential response of photosynthetic pigments, rubisco activity and rubisco protein of Arabidopsis thaliana EXPOSED TO UVB and OZONE. *Photochem. Photobiol.* **1995**, *62*, 727–735. [CrossRef]
34. Yakovleva, I.M.; Titlyanov, E.A. Effect of high visible and UV irradiance on subtidal Chondrus crispus: Stress, photoinhibition and protective mechanisms. *Aquat. Bot.* **2001**, *71*, 47–61. [CrossRef]
35. Hua, Q.; Liu, Y.-G.; Yan, Z.-L.; Zeng, G.-M.; Liu, S.-B.; Wang, W.-J.; Tan, X.-F.; Deng, J.-Q.; Tang, X.; Wang, Q.-P. Allelopathic effect of the rice straw aqueous extract on the growth of *Microcystis aeruginosa*. *Ecotoxicol. Environ. Saf.* **2018**, *148*, 953–959. [CrossRef]
36. Wang, G.J.; Zeng, F.L.; Song, P.; Sun, B.; Wang, Q.; Wang, J.Y. Effects of reduced chlorophyll content on photosystem functions and photosynthetic electron transport rate in rice leaves. *J. Plant Physiol.* **2022**, *272*, 153669. [CrossRef]

37. Kuczynska, P.; Jemiola-Rzeminska, M.; Nowicka, B.; Jakubowska, A.; Strzalka, W.; Burda, K.; Strzalka, K. The xanthophyll cycle in diatom *Phaeodactylum tricornutum* in response to light stress. *Plant Physiol. Biochem.* **2020**, *152*, 125–137. [CrossRef]
38. Strasser, R.J.; Tsimilli-Michael, M.; Srivastava, A. Analysis of the chlorophyll a fluorescence transient. In *Chlorophyll a Fluorescence: A Signature of Photosynthesis*; Papageorgiou, G.C., Ed.; Springer: Dordrecht, The Netherlands, 2004; pp. 321–362. [CrossRef]
39. Strasserf, R.J.; Srivastava, A. Govindjee Polyphasic chlorophyll *a* fluorescence transient in plants and cyanobacteria*. *Photochem. Photobiol.* **1995**, *61*, 32–42. [CrossRef]
40. Govindje, E. Sixty-Three Years Since Kautsky: Chlorophyll a Fluorescence. *Funct. Plant Biol.* **1995**, *22*, 131–160. [CrossRef]
41. Ma, Z.L.; Wang, C.X.; Qin, W.L.; Wang, M.; Chen, B.B.; Jia, Y.; Qin, Z.X.; Dai, C.J.; Yu, H.G.; Li, G.; et al. Inhibitory effects of *Prorocentrum donghaiense* allelochemicals on *Sargassum fusiformis* zygotes probed by JIP-test based on fast chlorophyll fluorescence kinetics. *Mar. Environ. Res.* **2021**, *170*, 105453. [CrossRef]
42. Kruger, G.H.J.; Tsimilli-Michael, M.; Strasser, R.J. Light stress provokes plastic and elastic modifications in structure and function of photosystem II in camellia leaves. *Physiol. Plant.* **1997**, *101*, 265–277. [CrossRef]